

BIONIC SHAPE DESIGN OF ELECTRIC LOCOMOTIVE AND AERODYNAMIC DRAG REDUCTION

Zhenfeng WU¹, Yanzhong HUO², Wangcai DING³, Zihao XIE⁴

^{1,2,3,4} School of Mechanical and Electrical Engineering, Lanzhou Jiaotong University, Lanzhou, China

Contact:

1) wzhf@mail.lzjtu.cn

Abstract:

Bionics has been widely used in many fields. Previous studies on the application of bionics in locomotives and vehicles mainly focused on shape optimisation of high-speed trains, but the research on bionic shape design in the electric locomotive field is rare. This study investigated a design method for streamlined electric locomotives according to the principles of bionics. The crocodiles were chosen as the bionic object because of their powerful and streamlined head shape. Firstly, geometric characteristic lines were extracted from the head of a crocodile by analysing the head features. Secondly, according to the actual size requirements of the electric locomotive head, a free-hand sketch of the bionic electric locomotive head was completed by adjusting the position and scale of the geometric characteristic lines. Finally, the non-uniform rational B-splines method was used to establish a 3D digital model of the crocodile bionic electric locomotive, and the main and auxiliary control lines were created. To verify the drag reduction effect of the crocodile bionic electric locomotive, numerical simulations of aerodynamic drag were performed for the crocodile bionic and bluff body electric locomotives at different speeds in open air by using the CFD software, ANSYS FLUENT16.0. The geometric models of crocodile bionic and bluff body electric locomotives were both marshalled with three cars, namely, locomotive + middle car + locomotive, and the size of the two geometric models was uniform. Dimensions and grids of the flow field were defined. And then, according to the principle of motion relativity, boundary conditions of flow field were defined. The results indicated that the crocodile bionic electric locomotive demonstrated a good aerodynamic performance. At the six sampling speeds in the range of 40–240 km/h, the aerodynamic drag coefficient of the crocodile bionic electric locomotive decreased by 7.7% on the average compared with that of the bluff body electric locomotive.

Key words:

electric locomotive, bionic, crocodile, aerodynamic drag, numerical simulation

To cite this article:

Wu, Z., Huo, Y., Ding, W., Xie, Z., 2018. Bionic shape design of electric locomotive and aerodynamic drag reduction. Archives of Transport, 48(4), 99-109. DOI: <https://doi.org/10.5604/01.3001.0012.8369>



1. Introduction

In 1960, an American military doctor, J. E. Steele, coined the term 'bionics' and presented its related concepts; hence, bionics is a discipline that is both ancient and young (Maier et al., 2013). Bionics studies the structure, function or working principle of an organism then makes a scientific analysis and summary. The conclusion is transplanted into engineering technology, which can improve or create new technical equipment. Bionic design does not only imitate creatures in terms of function but also pursues the harmonious relationship amongst humans, objects and nature. Bionic design is essentially a process of human creation (Yuan et al., 2017). Natural creatures have evolved over 3.5 billion years in accordance with the principle of 'survival of the fittest' in natural selection. In the 5 million years of human evolution, human beings constantly imitated nature to improve their production capacity in the way of observation, inspiration, imitation and innovation (Tong et al., 2017). Thus far, bionics has been applied in numerous cases, such as paddles imitating fins, camouflage clothing imitating the colour of butterflies, radars invented according to the echo location principle of bats, mechanical arms of excavators that were invented based on the forearms of mantises, sidewinder missiles inspired by the hot positioning capability of rattlesnakes and the solution of airfoil flutter that was devised according to the location of dragonfly pterostigma (Wang et al., 2016). Bionics has also been applied in locomotives and vehicles. The Japanese Shinkansen applied the shape of a kingfisher's beak to the design of a head car and successfully developed kingfisher bionic trains, which reduce aerodynamic drag by approximately 20%. By analysing Malay tigers' nose, eyes and forehead characteristics, Yi et al. (2012) designed the head car of the Malaysian multiple unit. Zhou et al. (2014) summarised the bionic design process of high-speed trains and completed a creative design of a high-speed train by extracting the modelling elements of a giant Chinese salamander's front face. Their simulation results showed that the aerodynamic drag coefficient of the giant salamander bionic train is 0.113. Du et al. (2014) discovered that the non-smooth grooves on the surface of sharks can hinder the instantaneous transverse flow caused by turbulence. They established the geometrical shape of bionic non-smooth grooves and used a numerical simulation method to reduce the aerodynamic drag

of high-speed trains by 6%. Inspired by the fierceness of great white sharks, Lu et al. (2017) proposed a bionic image design method for high-speed trains and discussed the trade-off between image representation and technical constraints in the design process. To reduce the aerodynamic noise of high-speed trains, Wang et al. (2014) designed a rhombic surface texture at the gas-solid interface of high-speed trains according to the surface structure of shark skin and established a noise analysis model. Compared with the maximum friction noise reduction of a smooth surface, the reduction of a texture with an optimal diagonal ratio is 24 dB, and the reduction with an optimal depth-to-side ratio is 20 dB. Previous studies on the application of bionics in locomotives and vehicles mainly focused on shape optimisation of high-speed trains to reduce aerodynamic drag and noise. Research on bionic drag reduction in the electric locomotive field is rare (Mindur, 2017). This work used the crocodile as a bionic study object. The head shape of electric locomotives was optimised according to the geometric characteristics of the crocodile's head. The aerodynamic drag and surface pressure distribution of the crocodile bionic electric locomotive were studied through numerical calculation.

The rest of this paper is organised as follows. The determination of the bionic object of an electrical locomotive and its detailed design process are discussed in Sections 2 and 3, respectively. Section 4 presents the aerodynamic drag calculation for bionic and bluff body electric locomotives. The calculation results and analysis of the aerodynamic drag of the two types of locomotives are discussed in Section 5. Section 6 provides the conclusions.

2. Determination of the bionic object

Electric locomotives are powered by electric energy from the catenary system or conductor rail, and they drag trains by using electric motors. The power of electric locomotives is generally higher than that of diesel locomotives. Therefore, electric locomotives are the first choice for pulling high-speed passenger and heavy-haul freight trains.

Electric locomotives should have a strong and powerful shape. Considering the continuous increase in locomotive speed, the locomotive head should also have a proper streamlined shape. In bionic design, the selected bionic objects should meet the specific functional requirements of the product. Birds or fast

aquatic animals are usually selected as bionic objects to streamline the appearance of electric locomotives. However, birds give an impression of lightness and fragility. Meanwhile, although the fastest creeping speed of crocodiles is approximately 14 km/h only, crocodiles can demonstrate astonishing speed when they rush to surprise their prey. Thus, crocodiles were selected as bionic objects in this study instead of birds due to their strong force.

Crocodiles are one of the most primitive animals, and they have evolved for approximately 200 million years. The evolution of the crocodile head is exquisite. The crocodile head is characterised by a long and tapered mouth and a strong and powerful jaw. The nose is at the tip of the mouth, and the eyes are above the upper jaw. These raised shapes ensure that crocodiles only expose their eyes and nose above the water when hunting, which perfectly preserves their concealment.

The running of trains is bi-directional, but there is no suitable bionic equivalent. Therefore, both the head and tail of the locomotive took the crocodile's head as the bionic object, which was in line with the symmetrical shape characteristics of locomotives. By analysing the features of the crocodile's head, we extracted the geometric feature lines of the upper jaw, lower jaw, nose and eyes for the head shape design of the electric locomotive. The extracted feature lines are shown in Figure 1.



Fig. 1. Extracted feature lines of the crocodile's head

3. Detailed design process

The detailed design plan of the electric locomotive was completed after the geometric feature lines of the bionic object of the electric locomotive were determined. The process included drawing sketches, creating 3D digital models and visual rendering.

3.1. Free-hand sketch

In free-hand design, the designer manually draws the sketch without any mechanical equipment. Free-hand design reduces the design time and makes the design process highly flexible. Therefore, in the initial stage of creative expression of the product, the designer usually needs to draw many sketches to display the product from different perspectives. Then, the free-hand design that best fits the product positioning is selected.

The position and scale of the geometric characteristic lines of the bionic object should be adjusted according to the actual size requirements of the electric locomotive head. The geometric feature lines of the crocodile jaw must be straightened because the bottom of electric locomotives must be flat. In addition, the eyes of the crocodile are located on both sides above the upper jaw, but the front window of the electric locomotives cannot be set apart because they are used by the driver to see road lines and signs. Therefore, the characteristic lines of the crocodile's eyes should be moved to the centre, thus forming the front window of the electric locomotive. The free-hand design of the crocodile bionic electric locomotive obtained after multiple screening is shown in Figure 2.

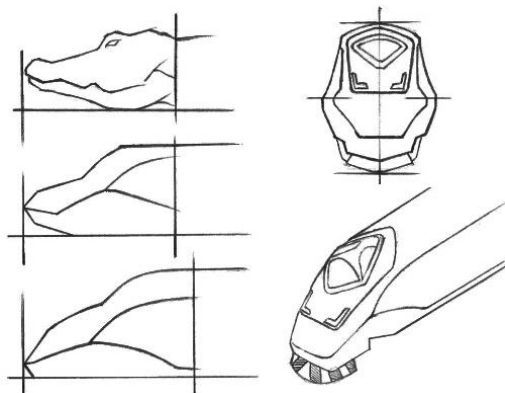


Fig. 2. Free-hand design of the crocodile bionic electric locomotive

3.2. Main control lines of locomotive

To evaluate and optimise the design from different perspectives, a 3D digital model of the crocodile bionic electric locomotive was established after the completion of the sketch design, that is, the 2D sketch was transformed into a 3D model. According to the selected sketch design, the main control lines

of the locomotive head were traced with the function of the non-uniform rational B-splines (NURBS) curve in the 3D design software CATIA V5R20, including longitudinal symmetry control, maximum cross-sectional, maximum overlooking control, and adjustable lines. Then, the positions of the control points in the space were changed to adjust the shape of the NURBS curve and make them closer to those in the sketch design. Half of the main control lines of the crocodile bionic electric locomotive in the longitudinal direction are shown in Figure 3.

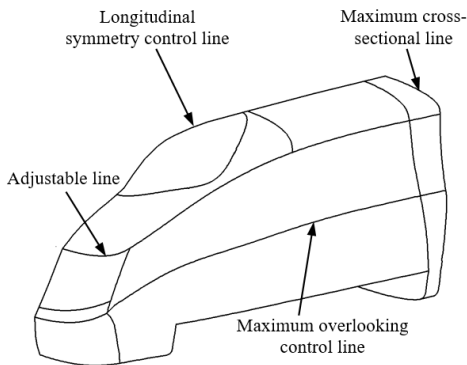


Fig. 3. Main control lines of the crocodile bionic electric locomotive head

The surface transition of the locomotive head should be natural, and the surface of the region with a large curvature change must avoid unsmooth phenomena, such as indentation and distortion. Thus, several auxiliary control lines need to be created between main control lines to complete the next surface filling. Half of the auxiliary control lines of the crocodile bionic electric locomotive in the longitudinal direction are shown in Figure 4.

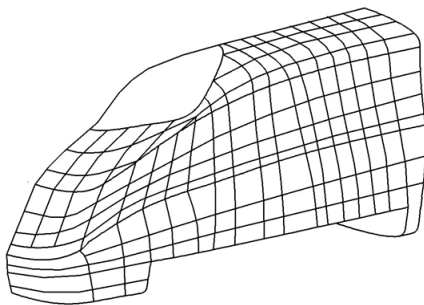


Fig. 4. Auxiliary control lines of the crocodile bionic electric locomotive head

The completed main and auxiliary control lines were connected through curved surface bridging, and the curvatures were adjusted appropriately to smoothen the connection between curves easily. For the regions with a large curvature change, the combination of curved surface bridging and surface filling may be used to ensure the quality of the surfaces. The filled surfaces of the crocodile bionic electric locomotive are shown in Figure 5.



Fig. 5. Surfaces of the crocodile bionic electric locomotive head

A flat roof was adopted for the locomotive body to facilitate the installation of roof equipment. Covered transition was used between the roof and side walls. A drum shape was employed for the side walls to reduce the aerodynamic drag and relieve the pressure pulse and lateral drag when trains pass each other. The 2D cross section of the car body of the crocodile bionic electric locomotive is shown in Figure 6.

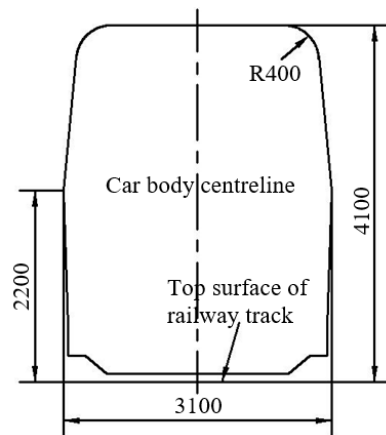


Fig. 6. Cross section of the car body of the crocodile bionic electric locomotive (unit: mm)

The crocodile bionic electric locomotive must be visually rendered properly to display the design results effectively. After many evaluations and discussions, white was set as the main colour and grey as the auxiliary colour. To enhance the visual impact of the locomotive, blue stripes were placed on the side walls for decoration. The rendering of the crocodile bionic electric locomotive is shown in Figure 7.



Fig. 7. Rendering of the crocodile bionic electric locomotive

4. Numerical simulation of aerodynamic drag of bionic electric locomotive

Current methods in train aerodynamic drag research include model experiments, real vehicle experiments and numerical simulation. Model experiments, which apply the principle of relative motion and flow similarity, include wind tunnel, dynamic model and flume experiments. However, model experiments have shortcomings, such as high initial investment and long experiment cycle (Xiao et al., 2013). Real vehicle experiments are usually conducted on special rail lines. However, the car bodies are usually not allowed to be damaged in the experiment. Thus, inserting a measuring wire into the vehicle is difficult. Meanwhile, numerical simulation has been widely applied to examine the aerodynamic performance of trains due to the continuous development of computer technology. Numerical simulation technologies mainly involve the application of professional numerical calculation software and the improvement of the numerical calculation method. Computational fluid dynamics (CFD) uses discretisation methods that can simulate and analyse various

problems of fluid dynamics. It has become an important means to solve all types of aerodynamic performance (Baker, 2010; Khier et al., 2000; Sloboda et al., 2016).

To verify the drag reduction effect of the crocodile bionic electric locomotive, numerical simulations of aerodynamic drag were performed for the crocodile bionic and bluff body electric locomotives at different speeds in open air by using the CFD software, ANSYS FLUENT16.0.

4.1. Geometric model

The geometric model was marshalled with three cars, namely, locomotive + middle car + locomotive. The head and rear locomotives had the same dimensions and external shape. The locomotive and the vehicle were connected by couplers. The bluff body electric locomotive used for comparison was rendered, as shown in Figure 8.



Fig. 8. Rendering of the bluff body electric locomotive

The streamlined head of the bluff body electric locomotive was small, that is, 2.6 m in this research. The size of the two geometry models, including the length, width and height of the locomotives, the length of the middle car and the cross section of the car body, were uniform. Both locomotives can be fitted with the same pantograph, bogie and coupler. The raised parts mentioned above were removed from the geometric models of the two locomotives to reflect the external shape of the locomotives and improve the calculation speed. The simplified geometric models of the two locomotives are shown in Figures 9(a)–(b).

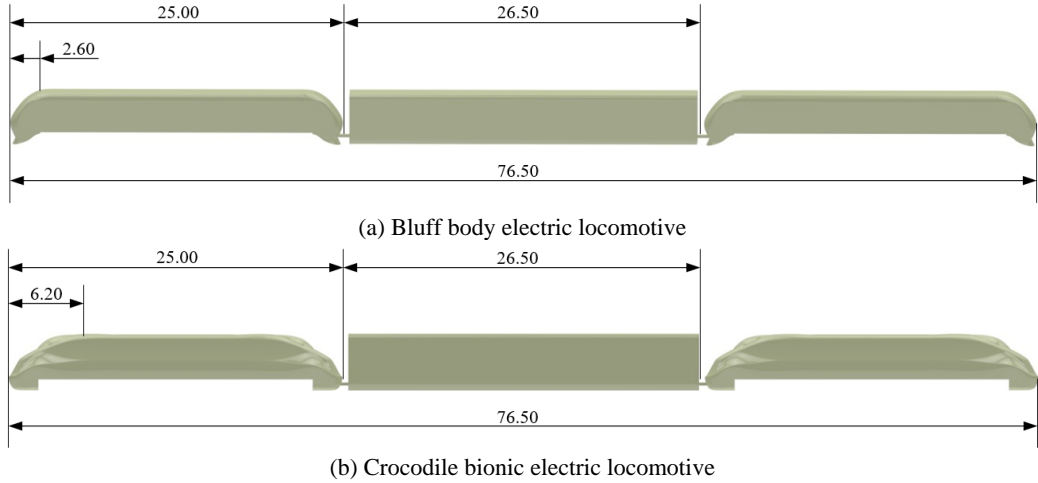


Fig. 9. Simplified geometric models (unit: m)

4.2. Mathematical model

When trains are running in open air, the train speed does not exceed 400 km/h. The effect of air density change on flow can be ignored without considering the train passing each other and the entering and exiting of tunnels. Therefore, the 3D constant incompressible viscous flow field can be used, and its control equations are expressed as follows (Paz et al., 2017; Tian, 2009):

$$\frac{\partial u_i}{\partial x_i} = 0, \quad (1)$$

$$\frac{\partial u_i}{\partial t} + u_j \frac{\partial u_i}{\partial x_j} = -\frac{1}{\rho} \frac{\partial p}{\partial x_i} + \frac{\mu}{\rho} \frac{\partial^2 u_i}{\partial x_j \partial x_j}. \quad (2)$$

In Equations (1)–(2), u_i, u_j represent the air velocity components of the flow field around the train. x_i, x_j represent the coordinate components, $i, j = 1, 2, 3$. ρ, p and μ represent the density, pressure and viscosity of air, respectively. t represents time.

The standard $k - \varepsilon$ turbulence model is a typical two-equation model, which is widely used in turbulence calculation. However, in the case of low Reynolds number, the calculation accuracy is unsatisfactory. Since the main research content of this paper is

the macroscopic flow field parameters of the trains, with a high Reynolds number, the standard $k - \varepsilon$ turbulence model was adopted to describe the flow field of the trains, and the relevant control equations can be defined as follows:

$$\frac{\partial(\rho k u_i)}{\partial x_i} = \frac{\partial}{\partial x_j} \left[\left(\mu + \frac{\mu_t}{\sigma_k} \right) \frac{\partial k}{\partial x_j} \right] + \mu_t \frac{\partial u_j}{\partial x_i} \left(\frac{\partial u_j}{\partial x_i} + \frac{\partial u_i}{\partial x_j} \right) - \rho \varepsilon, \quad (3)$$

$$\frac{\partial(\rho \varepsilon u_i)}{\partial x_i} = \frac{\partial}{\partial x_j} \left[\left(\mu + \frac{\mu_t}{\sigma_\varepsilon} \right) \frac{\partial \varepsilon}{\partial x_j} \right] + C_1 \mu_t \frac{\varepsilon}{k} \frac{\partial u_j}{\partial x_i} \left(\frac{\partial u_j}{\partial x_i} + \frac{\partial u_i}{\partial x_j} \right) - C_2 \rho \frac{\varepsilon^2}{k}. \quad (4)$$

In Equations (3)–(4), k represents the turbulent kinetic energy and ε represents the turbulent dissipation rate. μ_t represents the turbulent viscosity coefficient, and $\mu_t = C_\mu \rho k^2 / \varepsilon$. C_μ represents the turbulent constant. In general, $C_\mu = 0.09$. C_1, C_2, σ_k and σ_ε are empirical constants. In this study, $C_1 = 1.47, C_2 = 1.92, \sigma_k = 1.0$ and $\sigma_\varepsilon = 1.33$ (Bell et al., 2015; Wu et al., 2017).

4.3. Dimensions and grids of the flow field

The size of the outer flow field used the entire length ($L = 76.5$ m) of the geometric model as the characteristic length. The length of the inflow direction was $1L$, the lengths of the outflow and width directions were $2L$ and the height was $1L$. To save computing time and resources, the hybrid grid technique was used to discretise the computing area. A structured grid was adopted in the area near the car body, and an unstructured grid was adopted in the outer area of the car body (Jeong et al., 2015). In addition, the unstructured grid near the car body was refined to improve the accuracy of the calculation. The overall and local grids of the calculation domain are shown in Figures 10(a)–(b).

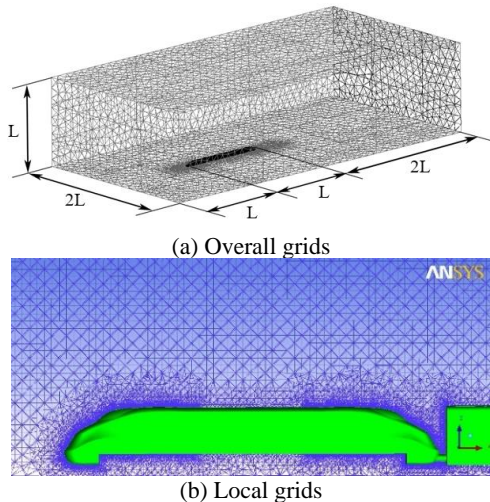


Fig. 10. Overall and local grids of the calculation domain

Grid division is an important part of flow field calculation. A high-quality computing grid was formed after several attempts. The geometrical dimensions and grid numbers of two models are listed in Table 1.

The main subject of the numerical simulations was aerodynamic drag performance of the trains, which was closely related to the surface pressure of the locomotives. Because the external dimensions of the two types of locomotive were the same, the crocodile bionic electric locomotive was adopted in the grid independence check. Two sampling points were

selected and named as point 1 and point 2, as shown in Figure 11.

Table 1. Geometrical dimensions and grid numbers of two models

Train type	Length(m)			Grids (million)
	Locomotive	Middle car	Geometric model	
Bluff body	25.00	26.50	76.50	2.66
crocodile bionic	25.00	26.50	76.50	2.72

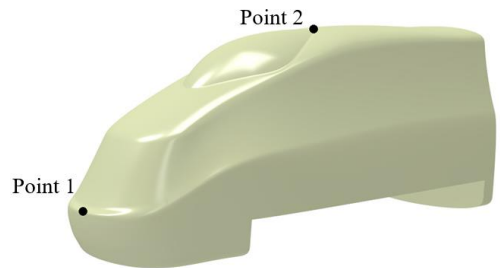


Fig. 11. The position of point 1 and point 2

The inlet velocity of the flow field was set as 120km/h. After many times of adjustment and calculation, we got the relationship between the grid number and the pressure at two points. As shown in Figure 12, when the grid number increased from 2.72 million to 5.10 million, the pressure changes of point 1 and point 2 were very small, indicating that the grid number of 2.72 million could meet the requirement of grid independence. Therefore, the grid number of the flow field was set as 2.72 million in the subsequent simulation.

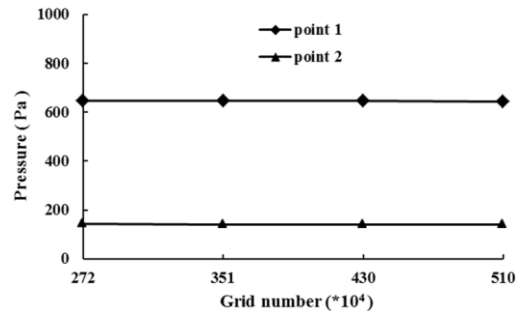


Fig. 12. Grid independence check

4.4. Boundary Conditions

The simulation process adopted the principle of motion relativity. Thus, the left side of the calculation domain was set as the speed inlet, and the right side was set as the pressure outlet, whose value was 1 standard atmospheric pressure. The sides and top of the calculating domain were set to symmetry boundaries, and the bottom of the calculation domain was set to the wall boundary (Zhang et al., 2016). The outer surfaces of trains were set to no-slip wall boundaries, the ground of the calculation domain was set to the slip wall boundary. The speed of the wall was set to the train speed, whose direction was opposite the flow velocity direction in front of the train, to simulate the relative motion between the train and ground (Oh et al., 2016).

5. Results and analysis

The surface pressure and path lines of the bluff body and crocodile bionic electric locomotives were calculated at a flow velocity of 120 km/h. In order to compare the results, dimensionless velocity coefficient and pressure coefficient were used. v_p represents the velocity coefficient of the path lines, and it can be expressed as follows:

$$v_p = \frac{v_1}{v_\infty} \tag{5}$$

In Equation (5), v_1 represents the velocity of the path lines; v_∞ represents the inflow velocity.

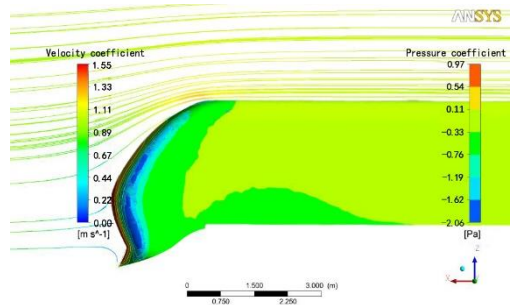
c_p represents the pressure coefficient of the train, and it can be expressed as follows:

$$c_p = \frac{p - p_\infty}{\frac{1}{2} \rho v_\infty^2} \tag{6}$$

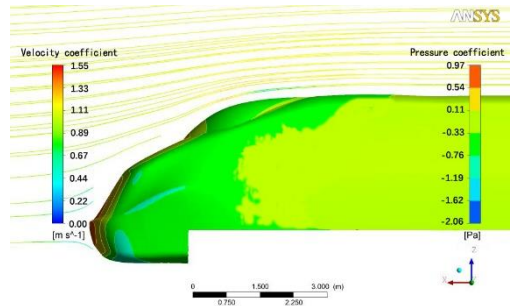
In Equation (6), p represents the static pressure on the surface of the train; p_∞ represents the atmospheric pressure; ρ represents the density of air. The calculated results are shown in Figures 13(a)–(b).

As shown in Figure 13, when the flow velocity was 120 km/h, the maximum velocity coefficients of the path lines of the two locomotives appeared in the transition of the head and roof. The value for the

bluff body electric locomotive was 1.55, and the value for the crocodile bionic electric locomotive was 1.38. The maximum pressure coefficients of the two locomotives appeared at the tip of the head. The pressure coefficient of the bluff body electric locomotive was 0.97, and the pressure coefficient of the crocodile bionic electric locomotive was 0.90. The calculation results indicated that the crocodile bionic electric locomotive had lower maximum velocity of the path lines and the maximum surface pressure compared with the bluff body electric locomotive.



(a) Bluff body electric locomotive



(b) Crocodile bionic electric locomotive

Fig. 13. Pressure coefficient and velocity coefficient of the two locomotives

To verify the aerodynamic drag characteristics of the crocodile bionic electric locomotive comprehensively, the flow velocities were set to 40, 80, 120, 160, 200 and 240 km/h. The aerodynamic drags of the bluff body and crocodile bionic electric locomotives were calculated. Generally, the aerodynamic drag of trains running on a rail consists of three main parts: differential pressure, frictional and interference drags. The pressure difference between the

head and tail of trains causes pressure drag, and the value of pressure drag is strongly related to the shape of the head and tail of trains. Frictional drag, which is caused by the viscosity of air, is the gas shear force acting on the body surface. The value of frictional drag is related to the length of trains and surface properties. The drag caused by the disturbance in the raised parts of the train, including the pantograph, bogie and coupler, is called interference drag (Wang et al., 2007). The raised parts, which can cause interference drag, were simplified in the geometric models of the two locomotives. Therefore, this work only calculated the pressure and frictional drags of the locomotives. For the sake of explanation, the bluff body electric locomotive is called type A, and the crocodile bionic electric locomotive is called type B. In order to compare the results, dimensionless differential pressure drag coefficient, frictional drag coefficient and total aerodynamic drag coefficient were used. C_d represents the differential pressure drag coefficient, and it can be expressed as follows:

$$C_d = \frac{F_d}{\frac{1}{2} \rho v^2 S} \quad (7)$$

C_f represents the frictional drag coefficient, and it can be expressed as follows:

$$C_f = \frac{F_f}{\frac{1}{2} \rho v^2 S} \quad (8)$$

C_x represents the aerodynamic drag coefficient, and it can be expressed as follows:

$$C_x = \frac{F_x}{\frac{1}{2} \rho v^2 S} \quad (9)$$

In Equation (7) - (9), F_d represents the differential pressure drag; F_f represents the frictional drag; F_x represents the total aerodynamic drag; v represents the velocity of trains; S represents the maximum cross-sectional area of the trains. The calculated aerodynamic drag coefficients of the two locomotives are listed in Table 2.

Table 2. Aerodynamic drag of the two locomotives

Speed (km/h)	Train type	Differential pressure drag coefficient	Frictional drag coefficient	Aerodynamic drag coefficient
40	A	0.95	0.08	1.03
	B	0.86	0.08	0.94
80	A	0.94	0.08	1.02
	B	0.86	0.08	0.94
120	A	0.92	0.08	1.00
	B	0.85	0.07	0.92
160	A	0.92	0.07	0.99
	B	0.85	0.07	0.92
200	A	0.90	0.07	0.97
	B	0.83	0.07	0.90
240	A	0.90	0.07	0.97
	B	0.83	0.07	0.90

The basic drag of trains can be expressed as follows:

$$F = a + bv + cv^2 \quad (10)$$

In Equation (10), $a + bv$ is usually considered the mechanical drag of trains. It is caused by the friction of vehicle bearing and the rolling, sliding and impact vibration between the wheels and the rail. The values of A and B are determined by real vehicle experiments, which are not studied in this paper. cv^2 is usually considered the aerodynamic drag caused by air. The relationship between c and C_x can be expressed as follows:

$$c = \frac{1}{2} \rho S C_x \quad (11)$$

To illustrate the drag coefficient reduction effect of the crocodile bionic electric locomotive intuitively, the speed-aerodynamic drag coefficient curves of types A and B are shown in Figure 14.

As shown in Figure 14, the speed-aerodynamic drag coefficient curves of the two types of locomotive are both approximately straight lines within the 40–240 km/h speed range, which indicates that two types of locomotive have relatively stable aerodynamic drag coefficient. The ratio of drag coefficient reduction was 8.7% at 40 km/h, 7.8% at 80 km/h, 8.0% at 120 km/h, 7.1% at 160 km/h, 7.2% at 200 km/h and 7.2% at 240 km/h. At the six sampling speeds in the range of 40–240 km/h, the aerodynamic drag coefficient of the crocodile bionic electric locomotive decreased by 7.7% on the average compared with that of the bluff body electric locomotive.

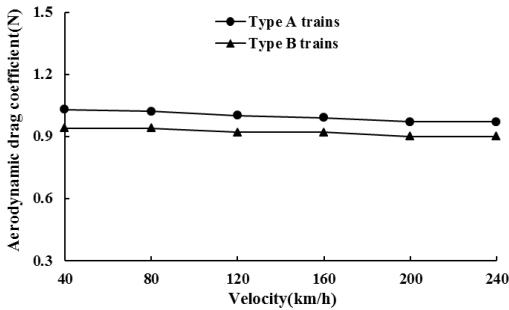


Fig. 14. Speed-aerodynamic drag coefficient curves of the two trains

6. Conclusion

From the biology perspective, bionics is a branch of applied biology. However, from the engineering perspective, bionics is the combination of the following two processes. Firstly, human beings find inspiration from evolving organisms in nature. Second, the study of organisms provides principles, methods or approaches for the design and construction of new technical equipment. Therefore, bionics mainly provides human beings with a reliable and efficient technology system that is similar to biological characteristics and can benefit mankind. This research on bionics design of electric locomotives explored the design of an optimal locomotive shape. Due to the limitation of the head size of electric locomotives, the position and scale of the geometric characteristic lines needed to be adjusted after selecting crocodiles as the bionic object.

The results of the numerical simulation of the bluff body and crocodile bionic electric locomotives indicated that the crocodile bionic electric locomotive can achieve a significant reduction in aerodynamic drag coefficient. In terms of manufacturing, the head shape of the crocodile bionic electric locomotive is more complicated than that of the bluff body electric locomotive. However, with the current equipment manufacturing capacity for locomotives and vehicles, the problem of manufacturing locomotive heads with complex shapes can be addressed permanently.

Acknowledgements

The work of this paper is supported by the National Natural Science Foundation of China (Grant No. 11462011, 51665027) and Xiaoping Science and Technology Innovation Team.

References

- [1] BAKER, C. J., 2010. The flow around high speed trains. *Journal of Wind Engineering and Industrial Aerodynamics*, 98(6/7), 266–298.
- [2] BELL, J. R., BURTON, D., THOMPSON, M. C., et al., 2015. Moving model analysis of the slipstream and wake of a highspeed train. *Journal of Wind Engineering and Industrial Aerodynamics*, 2015(136), 127-137.
- [3] DU, J., GONG, M., TIAN, A., et al., 2014. Study on the drag reduction of the high-speed train based on the bionic non-smooth riblets. *Journal of Railway Science and Engineering*, 11(5), 70-76.
- [4] JEONG, S. M., LEE, S. A., RHO, J. H., et al., 2015. Research of high-speed train pantograph shape design for noise and drag reduction through computational analysis. *Journal of Fluids Engineering*, 20(2), 67-72.
- [5] KHIER, W., BREUER, M., DURST, F., 2000. Flow structure around trains under side wind conditions: A numerical study. *Computers & Fluids*, 29(2), 179-195.
- [6] LU, J. N., XU, B. C., ZHI, J. Y., et al., 2017. Image bionic design of high speed train head modeling. *Journal of Machine Design*, 34(9), 106-110.
- [7] MAIER, M., SIEGEL, D., THOBEN, K., 2013. Transfer of natural micro structures to bionic lightweight design proposals. *Journal of Bionic Engineering*, 10 (4), 469-478.
- [8] MINDUR, L., 2017. Development of Italian railways in the period 2002-2015, including high-speed railway lines. *Scientific Journal of Silesian University of Technology. Series Transport*, 96, 115-127.
- [9] OH, H. K., KWON, H., KWAK, M., et al., 2016. Measurement and analysis for the upper side flow boundary layer of a high speed train using wind tunnel experiments with a scaled model. *Journal of the Korean Society for Railway*, 19(1), 11-19.
- [10] PAZ, C., SUAREZ, E., GIL, C., 2017. Numerical methodology for evaluating the effect of sleepers in the underbody flow of a high-speed train. *Journal of Wind Engineering and Industrial Aerodynamics*, 2017(167), 140-147.
- [11] SLOBODA, O., KORBA, P., HOVANEC, M., PILA, J., et al., 2016. Numerical approach in aeroelasticity. *Scientific Journal of Silesian*

- University of Technology. Series Transport*, 93, 115-122.
- [12] TIAN, H. Q., 2009. Formation mechanism of aerodynamic drag of high-speed train and some reduction measures. *Journal of Central South University of Technology*, 16(1), 166-171.
- [13] TONG, J., XU, S., CHEN, D., 2017. Design of a bionic blade for vegetable chopper. *Journal of Bionic Engineering*, 14 (1), 163-171.
- [14] WANG, D., ZHAO, W., MA, S., 2007. Application of CFD numerical simulation in high speed train design. *Journal of the China Railway Society*, 29(5), 64-68.
- [15] WANG, J. G., CHEN, S. H., WANG, Q. J., 2014. Effect of bionic rhombic surface texture on frictional noise of high-speed train. *Journal of Traffic and Transportation Engineering*, 14(1), 43-48.
- [16] WANG, Z., GAO, K., SUN, Y., 2016. Effects of bionic units in different scales on the wear behavior of bionic impregnated diamond bits. *Journal of Bionic Engineering*, 13 (4), 659-668.
- [17] WU, Z., YANG, E., DING, W., 2017. Design of large-scale streamlined head cars of high-speed trains and aerodynamic drag calculation. *Archives of Transport*, 44(4), 89-97.
- [18] XIAO, J. P., HUANG, Z. X., CHEN, L., 2013. Review of Aerodynamic Investigations for High Speed Train. *Mechanics in Engineering*, 35(2), 1-12.
- [19] YI, Q., MAO, R. X., ZHANG, S., 2012. Applications of bionic shaping design in industrial design of railway vehicles. *Electric Locomotives & Mass Transit Vehicles*, 35(3), 58-62.
- [20] YUAN, F., YUAN, E., IGNAT, M., ARDELEAN, I., 2017. A bionic study of the magnetic bacteria with applications to the mecano-magnetic micromanipulators. *Procedia Engineering*, 174,1128-1139.
- [21] ZHANG, J., LI, J., TIAN, H., et al., 2016. Impact of ground and wheel boundary conditions on numerical simulation of the high-speed train aerodynamic performance. *Journal of Fluids and Structures*, 2016(61), 249-261.
- [22] ZHOU, L. C., DAI, R., CHEN, X., 2014. The Application of Bionics Design in the Design of Chinese High Speed Train. *Design*, 2014(17), 57-58.